Complex III Mitochondrial Leukoencephalopathy Masquerading Acute Demyelinating Syndrome Due to a Novel Variant in *CYC1*

Erfan Heidari
Tarbiat Modares University https://orcid.org/0000-0002-8361-4096
Maryam Rasoulinezhad
Tehran University of Medical Sciences
Neda Pak
Tehran University of Medical Sciences
Mahmoud Reza Ashrafi
Tehran University of Medical Sciences
Morteza Heidari
Tehran University of Medical Sciences
Brenda Banwell
University of Pennsylvania
Masoud Garshasbi
Tarbiat Modares University
Ali Reza Tavasoli (a_tavasoli@sina.tums.ac.ir)
Tehran University of Medical Sciences https://orcid.org/0000-0003-0440-5809

Research

Keywords: CYC1, mitochondrial leukoencephalopathy, complex III deficiency, acquired demyelinating syndrome

Posted Date: February 23rd, 2021

DOI: https://doi.org/10.21203/rs.3.rs-224767/v1

Abstract

Background

Complex III (CIII) is the third out of five mitochondrial respiratory chain complexes residing at the mitochondrial inner membrane. The assembly of 10 subunits encoded by nuclear DNA and one by mitochondrial DNA result in the functional CIII which transfers electrons from ubiquinol to cytochrome c. Deficiencies of CIII are among the least investigated mitochondrial disorders and thus clinical spectrum of patients with mutations in CIII is not well defined.

Results

we report on a 10-year-old girl born to consanguineous Iranian parents presenting with acute neurological deficits reminiscent of acquired demyelination, mainly acute bilateral vision loss, who was ultimately confirmed to have a novel homozygous missense variant, c.949C>T; p.(Arg317Trp) in complex III of the mitochondrial chain. Sanger sequencing confirmed the segregation of this variant with disease in the family.

Conclusion

We present a patient with a mitochondrial leukoencephalopathy due to complex III deficiency that manifested with features suggestive of an acquired demyelinating syndrome. The effect of this variant on the protein structure was shown *in-silico*. Our findings, not only expand the clinical spectrum due to defects in *CYC1* gene but also highlight that mitochondrial disease should be considered in children with acute CNS demyelination.

Background

Leukodystrophies usually manifest with bilateral, confluent and symmetric abnormal white matter signal changes in brain magnetic resonance imaging (MRI) while asymmetric multifocal lesions usually address the acquired white matter disorders (1) An overlapping clinical and imaging presentations of mitochondrial leukoencephalopathy and acquired demyelinating disorders due to mutation in *LYRM7* coding for complex III has been reported (2). Ubiquinol–cytochrome c oxidoreductase or complex III (CIII) is a cardinal unit of mitochondrial oxidative phosphorylation chain, which together with other complexes within the inner membrane of mitochondria generate the required cellular ATP (3). Dimeric CIII fulfills its function by oxidation of the ubiquinol and dispatching the electron to cytochrome c (4). This process is mediated by a homodimeric structure ($CIII_2$) in which each functional monomer is composed of 10 nuclear encoded structural subunits and only one mitochondrial encoded subunit called as cytochrome *b* (CYB) (5, 6). CYB (with two b-type hemes), UQCRFS1 (Rieske protein, containing an Fe-s cluster) and cytochrome c_1 (cyt c_1, with one c type heme) form the redox core of CIII by possessing the obligate prosthetic groups (5).

The biogenesis and role of cyt c1 in CIII is well understood. It is synthesized as a pre-protein in the cytosol and post-translationally imported into mitochondria where it turns to its mature protein after two cleavage episodes (7). The matured protein with its covalently attached heme c1 at N terminal of the protein poses in a unique topology within the CIII and is functional to accept electrons from the Rieske protein and pass it to cytochrome *c* (7–9).

Despite the fact that the function of CIII structural proteins including cyt c_1 is well understood, the genotype-phenotype correlation of many of these proteins are yet to be classified. In general, defective complex III mitochondrial disease associates with a broad spectrum of clinical features including mild neurodevelopmental delay, failure of somatic growth, exercise intolerance, cardiomyopathy, encephalomyopathy, liver and kidney problems (10–12).

Here, we report the clinical and molecular findings of a 10-year-old female patient who presented with clinical manifestations of recurrent optic neuritis. Her CSF OCBs and white cell counts and rheumatologic laboratory findings were all negative. Based on serial MRI evidence of unusual brain and spinal imaging findings such as periaqueductal gray matter involvement or progressive optic nerve atrophy and basal ganglia involvement, which are atypical for acquired relapsing demyelination, mitochondrial leukoencephalopathy investigated. Whole exome sequencing (WES) confirmed the diagnosis of type III mitochondrial leukoencephalopathy by identifying a homozygous variant in *CYC1* gene.

Results

Clinical Presentation

A 10 year- old female patient was presented to the emergency room with the chief complaint of sudden visual deficit following mild upper respiratory tract infection and trivial fever. Visual deficit was first noticed in the left eye followed by involvement of the right eye as light perception from a one meter distance. Mild painful bilateral extraocular eye movement was noted. Visual deficits progressed to the level of light perception from a less than half meter distance over the following two days. Ophthalmologic consultation and Optical Coherence Tomography (OCT) measures revealed a peripheral retinal edema and increased thickness of the retinal nerve fiber layer (Fig. 1).

She had normal eye movements in both horizontal and vertical planes, and had sluggish pupil reaction to light without photophobia. A severe visual acuity impairment of the patient was detected based on the neurologic examination. Ophthalmic consultation reported a visual acuity of 2/20. Other cranial nerves (CN) include CN 7–12 were intact. The rest of the neurological examination was normal. She was treated with methylprednisolone pulse 20mg/kg for five days. By the fifth dose, her vision recovered significantly as she was able to count the fingers from at least 1.5-meter distance.

Visual Evoked Potential (VEP) showed a severe delayed response compatible with central involvement of visual pathway (Right eye: N75 = 80.9ms, p100 = 134.08ms; Left eye: N75 = 84.16ms, P100 = 136.64ms).

On CSF analysis protein: 200 mg/dl, lactate: 91mmol/l) Nl ≤ 20 mmol/l) and no WBC and RBC were detected. Serum antibody levels for myelin oligodendrocyte (MOG), Aquaporin 4 antibodies (AQP4) and N-methyl-D-aspartate receptor (NMDAR) antibodies and cerebrospinal fluid (CSF) analysis for oligoclonal band (OCBs), AQP4 and NMDAR Abs and cell counts were all normal. Blood lactate level was normal.

She was discharged from the hospital and was followed up by using maintenance dose of oral prednisolone 1–2 mg/kg for 4 months based on a local consensus. Visual acuity improved significantly and was reported 16/20 based on the ophthalmologist report. While the patient was treating with oral steroid she developed progressive right lower limb non-pitting and non-gravity dependent edema caused her to be admitted again. No clinical signs of arterial or venous occlusion (e.g. cyanosis, numbness, pulselessness, coldness or pain) were detected during admission at all. Doppler sonography of lower limbs' vessels for deep vein thrombosis and arterial occlusion were negative. She was diagnosed with lymphoedema.

Two years after the first episode of bilateral optic neuritis, she experienced the second episode of ON, which again was treated with methylprednisolone pulse. Visual acuity was reported as 2/20. The result of second VEP showed an increased VEP's parameters (Right eye: N75 = 100.5ms, p100 = 148ms; Left eye: N75 = 94.7ms, P100 = 146ms). Her vision was partially improved after a 5 days' course of intravenous corticosteroids (20 mg/kg/day). Visual acuity was recorded as 14/20, which allowed her to functionally do her school responsibilities and daily activities of life with the help of her mother. Two weeks later, her visual acuity was measured as 16/20. She was treated with oral prednisone for four months. Laboratory evaluations for FANA, dsDNA, C3, C4, CH50, antiphospholipid and anticardiolipin antibodies, HLAB5, B27, B51 and serum ACE level were normal or negative. Auditory brainstem response (ARB) was also normal.

The patient experienced the third episode of ON four months later, in the context of a high-grade fever. Visual testing revealed a visual acuity of 6/20, bilaterally. Methylprednisolone pulse in addition to intravenous immunoglobulin (IVIG) were tried for treatment, with minimal clinical response. Over the course of three weeks, during which time she was treated with oral steroid, her vision improved to 14/20. Metabolic studies showed that serum ammonia, thyroid function tests, urine organic acid profiles, metabolic screen (MS/MS) and acyl carnitine profile were completely normal. Blood and CSF lactate levels were again elevated at 87 and 55 mmol/l, respectively.

On physical examination in her last visit at 10 years of age, she was alert, with HC of 56 cm, weight of 45 kg and height of 131 cm. Skin was normal without any abnormalities. On limb examination, she had non-pitting right lower extremity edema. In neuro-ophthalmic exam she had normal fix and follow, normal vertical and horizontal gaze, normal pupils' reaction to light, mild optic atrophy and blurred disc margins. Other cranial nerves in addition to cerebellar tests were all within normal limit. Deep tendon reflexes (DTRs) were absent on both ankles but knees and upper extremity DTRs were normal (+ 2). Plantar reflexes were bilaterally downward and she had mild steppage gait with mild foot-drop. Her gross motor function based on Gross Motor Function Classification System (GMFCS) score was 2 out of 5. Her IQ test

based on Wechsler test was normal with good school performance. Nerve conduction velocity (NCV) study revealed a uniform demyelinating sensory motor polyneuropathy.

According to her developmental history, the only remarkable point in her infancy and childhood period was mild motor delay in a way that she finally achieved acceptable motor milestones in upper limit of the normal range for her age. She was the only child of a first cousin parent who born through Caesarian section at 39 weeks of gestation after an uneventful pregnancy. Birth weight and head circumference (HC) were 3200 grs and 34 cm, respectively. No family history of demyelinating disorders or metabolic disorders such as mitochondrial leukoencephalopathy was reported.

During the first patient's admission, brain and orbital MRI without and with Gadolinium-DTPA administration were performed using Philips Ingenia 1.5 Tesla MRI system. T1 and T2 weighted sequences in axial, coronal and sagittal planes, axial FLAIR and DWI and ADC map sequences were obtained for brain imaging, and coronal orbital STIR and T2 sequences, axial and coronal T1 sequence and post contrast T1 sequences (with and without fat suppression) were obtained for orbital imaging. Patchy hyper signal intensity of anterior optic pathway including chiasma, intracranial and intraorbital optic nerves were detected in T2-W images which were associated with abnormal contrast enhancement in T1-W post contrast images. There were also non-enhancing symmetric hypersignal foci on T2 and FLAIR sequences in both caudate nucleus heads and anterior aspect of putamina without restriction on DWI and ADC map sequences. Mild hyperintensity was also noted in periaqueductal region and periventricular white matter on axial FLAIR and T2 sequences. Global cerebral atrophic changes were present. (Fig. 2).

Orbital and brain MRI at the second admission showed some similar findings as the first one, but at this time, the abnormal signals of the optic pathway and brain had been faded by some degree. Contrast enhancement was depicted again which was denoting active white matter demyelination lesions along the anterior part of optic pathway. (Fig. 3)

On the third admission about 4 month after the second disease episode, a whole spinal MRI was also performed in which a long segment of increased T2 signal was detected in cervical cord involving mostly its posterior aspect. No spinal cord enhancement was seen. Brain and orbital MRI showed optic nerve atrophy and increased periventricular white matter signal alteration as well as thin chronic subdural effusion in left frontal extra-axial space were detected beside presence of previous changes (Fig. 4). Following confirmation of her mitochondrial disease diagnosis, she was prescribed vitamin B1, B2, Biotin, E, COQ10 and carnitine supplements. Her vision improved to 16/20 at the time of last examination.

Molecular Diagnosis and Results of WES

Whole exome sequencing, validation and in silico analysis

We performed WES in combination with mitochondrial genome sequencing to uncover the genetic etiology of affected proband. WES resulted in on-target sequences with a mean coverage of 100-fold, with 97% of targets covering at least 10-fold. 100% of the target base pairs of the mitochondrial genes were covered at least 1000-fold. The average cover was 20712-fold. Custom prioritization scheme was applied to find the pathogenic variant out of called exome and mitochondrial variants which ultimately led to the identification of a homozygous variant (NM_001916.4, c.949C > T) in *CYC1* gene. This missense variant [Chr8.GRCh37:g.145152210C > T, c.949C > T, p. (Arg317Trp)] was confirmed by Sanger sequencing and segregated in the family. No trace of this variant was found in any public variant databases and was predicted to be damaging by various in-silico pathogenicity prediction tools (Table 1). At the protein level, Arg317 showed a high level of conservation from Human down to yeast, suggesting a crucial role in the normal activity of the protein (Fig. 5a). Next, the protein structure was evaluated for any alteration in polar contacts, showing that Arg317 is in interaction with several residues (CYC1: Valine313, Leu314, UQCRB: Lys72 and MT-CYB: Asp216). It was observed that interaction with Asp216 will be lost as a result of p. (Arg317Trp) variant and a new interaction will be generated between tryptophan and Lue19 of cytochrome b-c1 complex subunit 8 (UQCRQ). Protein structure of cyt *c1* within the CIII and interactions of the wild type and mutant residue are shown in Fig. 5b and 5c, respectively.

Table 1
Nuclear, mitochondrial and assembly components of responsible genes encoding COM III of OXPHOS complex.

OXPHOS Component	Complex III	Clinical Symptoms	Lab/Imaging Findings	Ref
mtDNS subunit genes	MTCYB	Persistent vomiting, weight loss and diarrhea, Metabolic decompensation, Exercise intolerance and MELAS-like spectrum	lactic acidosis, hypoglycemia, elevated liver enzymes and CPK[3], high lactate level in UOA[4] profile, ↑ lactate band in MRS[5]	(10, 18, 19)
Nuclear subunit genes	UQCRB	Metabolic decompensation following gastroenteritis	Lactic acidosis, Hypoglycemia	(20)
	UQCRC2	Neonatal encephalopathy, Metabolic decompensation following febrile illness, Neurologic regression	Lactic acidosis, Hypoglycemia, Hyperammonemia	(21)
	UQCRQ	Severe psychomotor retardation, Movement disorder, Myopathy	Mild to severe lactic acidosis, Abnormal BG[2] signals	(22)
	CYC1	Vomiting following fever	Recurrent lactic acidosis, Insulin-responsive hypoglycemia	(8)
Assembly/Ancillary Proteins	BCS1L	kidney and liver problems, bilateral cataract, FTT, hair and hearing problems, GRACILE[1] syndrome, Chronic encephalopathy and CP mimicker	Lactic acidosis, Hyperammonemia, Cerebral atrophy and WM/BG[2] signal changes	(12, 23–25)
	LYRM7	Motor problems, Neurologic regression and encephalopathy following fever, Pyramidal signs, FTT, ADS	Cavitating Leukoencephalopathy, Lactic acidosis	(11, 26, 27)
	UQCC2	Neonatal encephalopathy, Renal tubulopathy	Lactic acidosis	(3)
	UQCC3	Eating and sleep problems in neonatal period, psychomotor delay, motor weakness	Recurrent lactic acidosis, Hypoglycemia,	(4)
	TTC19	Early to late onset neurodegeneration, Ataxia, motor problems, psychiatric symptoms,	Lactic acidosis, Abnormal WM signal in BG, medulla and cerebellum,	(28–30)

Table 2
Identified CYC1 variant and evaluation of its pathogenicity using online prediction tools

Variant	Gene/genomic location	Allele Frequencies	Effect
NM_001916.4:c.949C > T Arg317Trp	*CYC1*: Chr8(GRCh37): g.145152210C > T	gnomAD: NR	PROVEAN: Damaging
		1000 Genome: NR	Mutation Taster: Disease causing
		ESP: NR	FATHMM-MKL: Damaging
		Iranome: NR	SIFT: Damaging

To analyze the downstream effects of the p. (Arg317Trp) variant on Cytochrome C1 protein structure stability, MUPro (Cheng et al., 2005) were employed. The obtained result indicated that the variant decreases the stability of cyt c_1 protein structure.

Discussion

We report a 10-year-old girl with recurrent episodes of profound visual loss, partially responsive to corticosteroids, who also manifested with brain MRI features of mitochondrial disease (abnormal signal in the basal ganglia and progressive atrophy), abnormal spinal cord signal, and peripheral motor-sensory neuropathy. Although her initial presentation with acute bilateral visual loss led to her diagnosis of acquired demyelinating optic neuritis, the profound nature of her visual loss was atypical. Profound visual loss can occur in patients with antibodies directed against AQP4, and to a lesser degree, in patients with antibodies against MOG. Patients with optic neuritis in the context of multiple sclerosis rarely have profound visual loss at onset. Given these features, as well as the development of MRI findings that were bilateral, relatively symmetric, and involving brain regions of high metabolic demand, the possibility of mitochondrial disease was suspected. Findings of peripheral neuropathy also argued against an acquired central nervous system demyelinating process. Her diagnosis was confirmed by comprehensive genetic analysis.

The products of several nuclear-encoded genes (*UQCRB*, *UQCRC1*, *UQCRC2*, *CYC1*, *UQCRFS1*, *UQCRH*, *UQCRQ*, *UQCR10*, *UQCR11*) and one mitochondrial-encoded gene (*MT-CYB*) form the primary subunits of the CIII which ultimately congregated by different assembly factors (*BCS1L*, *LYRM7*, *TTC19*, *UQCC1*, *UQCC2*, *UQCC3*) resulting in the functional homodimer CIII (9, 13).

Cytochrome c1 (cyt c_1) is a protein of the mitochondrial inner membrane which mainly consists of a polypeptide chain residing in mitochondrial intermembrane space and a helical hairpin structure anchoring the protein to phospholipid bilayer of inter membrane (7, 14). A short stretch of amino acids is protruded from this helical structure to the matrix. To our knowledge, no specific function is attributed to this segment and its role in the protein stability has not been defined yet.

Here, we identified a novel missense variant, c.949C > T; p.(Arg317Trp), in *CYC1* gene in a 10-year-old female patient suspected to mitochondrial disorder who was clinically unresponsiveness to recurrent ON treatment. Arg317 is located at the C terminal of the cyt c_1 protein and possess a high level of conservation from human to yeast. Several in-silico pathogenicity evaluators predicted that this variant is highly deleterious for the protein function. To further verify this predictions, we analyzed the recent Cryo-EM structure of human CIII (15). It enabled us to postulate that how the identified variant might lead to the state of the disease. This residue is placed at the starting point of the flanking stretch of amino acids within the mitochondrial matrix and is in interaction with several residues of the same protein and other neighbor proteins (cytochrome b-c1 complex subunit 7 and cytochrome b). The substituted tryptophan losses the contact with cytochrome b and gain a novel interaction with cytochrome b-c1 complex subunit 8. Although these interactions are not ranked as the strongest interactions but this in-silico prediction could suggest dysfunction of protein interaction as a probable mechanism. In future, functional studies and in-situ experimental approaches are needed to investigate the impact of this variant on protein function and complex III activity.

A wide range of clinical manifestations have been reported in association with mutations in genes encoding protein components of complex III of the respiratory complex (Table 1) (8, 15–27). Metabolic decompensation following a febrile illness, motor and growth problems, psychomotor delay, neurologic regression and psychiatric symptoms have been reported. The age of onset varies from neonatal to adulthood period. None of these neurologic and non-neurologic problems were observed in our patient before the onset of vision problem at the age of 10 years old.

Recurrent optic neuritis has not been reported, to our knowledge, in patients with *CYC1* mutations, nor in patients with mutations in other genes responsible for normal function of CIII. However, recurrent optic neuropathy is a feature of other mitochondrial disorders, such as Leber's Hereditary Optic Neuropathy (LHON) and in patients with mitofusin mutations. In addition, acute neurological deficits with MRI features of white matter abnormalities in the brain and spinal cord have been reported in CI deficiency, CIII deficiency due to *LYRM7* mutations, mtDNA depletion syndrome and multiple mitochondrial dysfunction syndrome (2). On the other hand, a preliminary assumption of the appearance of demyelination-like lesions such as multiple sclerosis has been proposed in some mitochondrial genomic haplotype variation (16). These findings suggest common boundaries between acquired demyelinating syndromes and mitochondrial leukoencephalopathies but needs further investigations.

Conclusion

In conclusion, we emphasize the importance of considering mitochondrial disorders in the differential of acquired demyelination in children. To our knowledge, this is the second variant reported in *CYC1* gene as cause of aforementioned phenotypes.

Material And Methods

Ethical approval and consent

Approval of this study was obtained from the ethics review board at Children's Medical Center (CMC) hospital and Tarbiat Modares Univeristy (TMU) of Tehran, Iran. The understudy family sought medical counselling at Myelin Disorders Clinic, CMC hospital and then referred to Medical genetics department of TMU for genetic investigation. Proper informed consent was obtained and parents were ensured to be informed of the result of this study.

Exome sequencing and data analysis

DNA was extracted from the index patient and her healthy family members using Roche extraction kit (Product No. 11814770001). After quality assessment of extracted DNA, all coding region of the index patient was baited against exonic regions and flanking exon-intron boundary regions of the genome utilizing Agilent's Sure Select Human All Exon V6 kit (Agilent, SantaClara, CA, USA). Paired-end sequencing was performed on Illumina's HiSeq4000 instrument in accordance to the manufacturer's protocols (Illumina Inc, USA). Obtained raw reads from sequencing machine were initially aligned onto human genome reference (NCBI build37/hg19 version) using BWA 0.7.17 after removing low quality reads. Afterward, reads were mark duplicated by implementing PICARD software 2.2 and variants (SNPs and Indels) were called utilizing Genome Analysis Toolkit 4.1. Annotations were incorporated to the called variants using ANNOVAR (17).

Prioritization of variants was applied based on a custom scheme. Given the consanguinity of parents, heterozygous variants were ruled out. Exclusion of intragenic, UTRs regions, intronic and synonymous variants was done and followed by opting variants with less than 1% minor allele frequency using 1000 Genomes Project, dbSNPv152, Exome Sequencing Project (ESP), Exome Aggregation Consortium (ExAC) database and Exome Variant Server. Then, further evaluations on the influence of the variants on protein function according to pathogenicity evaluator tools were performed (Mutation Taster, SIFT, Provean, Polyphen-2, MutPred2, and M-CAP). Genotype-phenotype correlation of variants and their relation to patient's phenotype was checked in ClinVar and HGMD. Website addresses for online tools or software for pathogenicity prediction, and protein modeling are provided at the end of this article.

Mitochondrial Genome Sequencing

Targeted amplification of the entire mitochondrial genome was done using two overlapping long range PCRs. The amplicons were run on the Bioanalyzer to assess for any putative deletion within the mitochondrial genome. The amplified products were subsequently segmented and Illumina compatible adapters ligated to generate libraries that were sequenced on an Illumina HiSeq4000 HiSeq4000 platform to an average sequencing depth of 1000x.

Raw sequence data analysis, including base calling, demultiplexing, alignment to the Revised Cambridge Reference Sequence (rCRS) of the Human Mitochondrial DNA (NC_012920) and variant calling were performed using a validated in-house software. Following the base calling and primary filtering of low

quality reads, standard Bioinformatics pipeline was implemented to annotate detected variants and to filter out probable artefacts. The pipeline confidently detects heteroplasmy levels down to 15%. All identified variants were evaluated with respect to their pathogenicity and causality.

Sanger sequencing

Sanger sequencing was performed for verification and family segregation on the final candidate variants. We also evaluated the presence of these variants in a cohort of ethnicity-matched controls. The bidirectional primers listed in Supplementary Table 1 were utilized for PCR amplification of the variant region. Cycling conditions were including the initial denaturation (94°C, 3min) followed by 40 cycles of 94°C for 30s, 64°C for 30s, 72°C for 30s, and a final extension at 72°C for 10min. Consequently, PCR products were visualized by electrophoresis using 1.5% agarose gel and PCR products were sequenced utilizing the ABI 3130xl Genetic Analyzer. Sequencing chromatograms were analyzed using the SnapGene v.5.0.5 software.

Protein structure, stability and conservation

The study of the affected residue was conducted by employing the available human CYC1 structure (PDB ID: 5XTE), as reported by Guo et al (2017). The PDB file was investigated for possible polar contact changes upon mutation by PyMOL software (The PyMOL Molecular Graphics System, Version 2.3.2, Schrödinger, LLC). The effect of the identified variant on CYC1 Protein stability was estimated using MUPro (Cheng, Randall, & Baldi, 2005). ConSurf and UCSC databases were recruited to provide an evolutionary conservation profile for cyt *c1* protein.

Web resources

dbSNP152 (http://www.ncbi.nlm.nih.gov/snp)

Picard (http://picard.sourceforge.net)

1000 Genome Database (http://www.1000genomes.org/)

Clinvar (https://www.ncbi.nlm.nih.gov/clinvar)

gnomAD (http://gnomad.broadinstitute.org)

EVS (http://evs.gs.washington.edu/EVS).

Pymol software (https://pymol.org/2/)

SIFT&Provean (http://provean.jcvi.org)

GATK (http://www.broadinstitute.org/gatk/)

ExAC Browser (http://exac.broadinstitute.org)

dbSNP152 (http://www.ncbi.nlm.nih.gov/snp)

MutationTaster (http://www.mutationtaster.org)

Mutpred2 (http://mutpred.mutdb.org)

Consurf (http://www.consurf.tau.ac.il)

UCSC (https://genome.ucsc.edu)

NCBI (https://www.ncbi.nlm.nih.gov)

OMIM (https://omim.org/)

Poyphen-2 (http://genetics.bwh.harvard.edu/pph2/)

Clinvar (https://www.ncbi.nlm.nih.gov/clinvar)

HGMD (http://www.hgmd.cf.ac.uk)

Declarations

Ethics approval and consent to participate

The ethical committee of Children's Medical Center (CMC) hospital and Tarbiat Modares Univeristy approved the current study and written informed consent was obtained from patient's family prior to initiation of the experiments.

Consent for publication

All participants to this study were informed about the publication of genetic and clinical data of affected individual.

Availability of data and materials

The identified variant and phenotypes were submitted to ClinVar (Scv001245475). The Whole exome sequencing dataset used and analyzed in the current study is available from the corresponding author on reasonable request.

Competing interests

Not Declared

Author contributions

Designed the project: AT, MRA, BB; Genetic data collection & analysis: M.G, EH; Radiologic data collection & analysis: NP; Clinical evaluation: A.R.T, MRA, MR, MH; Initial draft: E.H, M.G., A.R.T, Critical Review: BB, ART, MG. All authors read and approved the final manuscript.

Acknowledgments

Our most special thanks go to the patients and their families who consented to be a part of this study. Myelin Disorders Clinic and Tarbiat Modares clinical and genetic research received no specific grant from any funding agency, commercial or not for profit sectors.

References

1. Ashrafi MR, Tavasoli AR. Childhood leukodystrophies: A literature review of updates on new definitions, classification, diagnostic approach and management. Brain Dev. 2017;39(5):369-85.
2. Bindu PS, Sonam K, Chiplunkar S, Govindaraj P, Nagappa M, Vekhande CC, et al. Mitochondrial leukoencephalopathies: a border zone between acquired and inherited white matter disorders in children? 2018;20:84-92.
3. Tucker EJ, Wanschers BF, Szklarczyk R, Mountford HS, Wijeyeratne XW, van den Brand MA, et al. Mutations in the UQCC1-interacting protein, UQCC2, cause human complex III deficiency associated with perturbed cytochrome b protein expression. PLoS Genet. 2013;9(12):e1004034.
4. Wanschers BF, Szklarczyk R, van den Brand MA, Jonckheere A, Suijskens J, Smeets R, et al. A mutation in the human CBP4 ortholog UQCC3 impairs complex III assembly, activity and cytochrome b stability. Hum Mol Genet. 2014;23(23):6356-65.
5. Conte A, Papa B, Ferramosca A, Zara VJBeBA-MCR. The dimerization of the yeast cytochrome bc1 complex is an early event and is independent of Rip1. 2015;1853(5):987-95.
6. Hunte C, Palsdottir H, Trumpower BL. Protonmotive pathways and mechanisms in the cytochrome bc1 complex. FEBS Lett. 2003;545(1):39-46.
7. Smith PM, Fox JL, Winge DRJBeBA-B. Reprint of: Biogenesis of the cytochrome bc1 complex and role of assembly factors. 2012;1817(6):872-82.
8. Gaignard P, Menezes M, Schiff M, Bayot A, Rak M, Ogier de Baulny H, et al. Mutations in CYC1, encoding cytochrome c1 subunit of respiratory chain complex III, cause insulin-responsive hyperglycemia. Am J Hum Genet. 2013;93(2):384-9.
9. Mukherjee S, Ghosh A. Molecular mechanism of mitochondrial respiratory chain assembly and its relation to mitochondrial diseases. Mitochondrion. 2020;53:1-20.
10. Dumoulin R, Sagnol I, Ferlin T, Bozon D, Stepien G, Mousson BJM, et al. A novel gly290asp mitochondrial cytochromebmutation linked to a complex III deficiency in progressive exercise intolerance. 1996;10(5):389-91.
11. Invernizzi F, Tigano M, Dallabona C, Donnini C, Ferrero I, Cremonte M, et al. A Homozygous Mutation in LYRM 7/MZM 1 L Associated with Early Onset Encephalopathy, Lactic Acidosis, and Severe

Reduction of Mitochondrial Complex III Activity. 2013;34(12):1619-22.

12. Ramos-Arroyo MA, Hualde J, Ayechu A, De Meirleir L, Seneca S, Nadal N, et al. Clinical and biochemical spectrum of mitochondrial complex III deficiency caused by mutations in the BCS1L gene. Clin Genet. 2009;75(6):585-7.
13. Alston CL, Rocha MC, Lax NZ, Turnbull DM, Taylor RW. The genetics and pathology of mitochondrial disease. J Pathol. 2017;241(2):236-50.
14. Gasser SM, Ohashi A, Daum G, Bohni PC, Gibson J, Reid GA, et al. Imported mitochondrial proteins cytochrome b2 and cytochrome c1 are processed in two steps. Proc Natl Acad Sci U S A. 1982;79(2):267-71.
15. Guo R, Zong S, Wu M, Gu J, Yang M. Architecture of Human Mitochondrial Respiratory Megacomplex I2III2IV2. Cell. 2017;170(6):1247-57 e12.
16. Mao P, Reddy PHJBeBA-MBoD. Is multiple sclerosis a mitochondrial disease? 2010;1802(1):66-79.
17. Wang K, Li M, Hakonarson H. ANNOVAR: functional annotation of genetic variants from high-throughput sequencing data. Nucleic Acids Res. 2010;38(16):e164.
18. Emmanuele V, Sotiriou E, Rios PG, Ganesh J, Ichord R, Foley AR, et al. A novel mutation in the mitochondrial DNA cytochrome b gene (MTCYB) in a patient with mitochondrial encephalomyopathy, lactic acidosis, and strokelike episodes syndrome. J Child Neurol. 2013;28(2):236-42.
19. Mori M, Goldstein J, Young SP, Bossen EH, Shoffner J, Koeberl DDJMg, et al. Complex III deficiency due to an in-frame MT-CYB deletion presenting as ketotic hypoglycemia and lactic acidosis. 2015;4:39-41.
20. Haut S, Brivet M, Touati G, Rustin P, Lebon S, Garcia-Cazorla A, et al. A deletion in the human QP-C gene causes a complex III deficiency resulting in hypoglycaemia and lactic acidosis. Hum Genet. 2003;113(2):118-22.
21. Miyake N, Yano S, Sakai C, Hatakeyama H, Matsushima Y, Shiina M, et al. Mitochondrial complex III deficiency caused by a homozygous UQCRC2 mutation presenting with neonatal-onset recurrent metabolic decompensation. Hum Mutat. 2013;34(3):446-52.
22. Barel O, Shorer Z, Flusser H, Ofir R, Narkis G, Finer G, et al. Mitochondrial complex III deficiency associated with a homozygous mutation in UQCRQ. Am J Hum Genet. 2008;82(5):1211-6.
23. Fernandez-Vizarra E, Bugiani M, Goffrini P, Carrara F, Farina L, Procopio E, et al. Impaired complex III assembly associated with BCS1L gene mutations in isolated mitochondrial encephalopathy. Hum Mol Genet. 2007;16(10):1241-52.
24. Hinson JT, Fantin VR, Schönberger J, Breivik N, Siem G, McDonough B, et al. Missense mutations in the BCS1L gene as a cause of the Björnstad syndrome. 2007;356(8):809-19.
25. Kasapkara CS, Tumer L, Ezgu FS, Kucukcongar A, Hasanoglu A. BCS1L gene mutation causing GRACILE syndrome: case report. Ren Fail. 2014;36(6):953-4.
26. Dallabona C, Abbink TE, Carrozzo R, Torraco A, Legati A, van Berkel CG, et al. LYRM7 mutations cause a multifocal cavitating leukoencephalopathy with distinct MRI appearance. Brain. 2016;139(Pt

3):782-94.
27. Hempel M, Kremer LS, Tsiakas K, Alhaddad B, Haack TB, Löbel U, et al. LYRM7-associated complex III deficiency: a clinical, molecular genetic, MR tomographic, and biochemical study. 2017;37:55-61.
28. Ghezzi D, Arzuffi P, Zordan M, Da Re C, Lamperti C, Benna C, et al. Mutations in TTC19 cause mitochondrial complex III deficiency and neurological impairment in humans and flies. Nat Genet. 2011;43(3):259-63.
29. Mordaunt DA, Jolley A, Balasubramaniam S, Thorburn DR, Mountford HS, Compton AG, et al. Phenotypic variation of TTC19-deficient mitochondrial complex III deficiency: a case report and literature review. Am J Med Genet A. 2015;167(6):1330-6.
30. Nogueira C, Barros J, Sa MJ, Azevedo L, Taipa R, Torraco A, et al. Novel TTC19 mutation in a family with severe psychiatric manifestations and complex III deficiency. Neurogenetics. 2013;14(2):153-60.

Figures

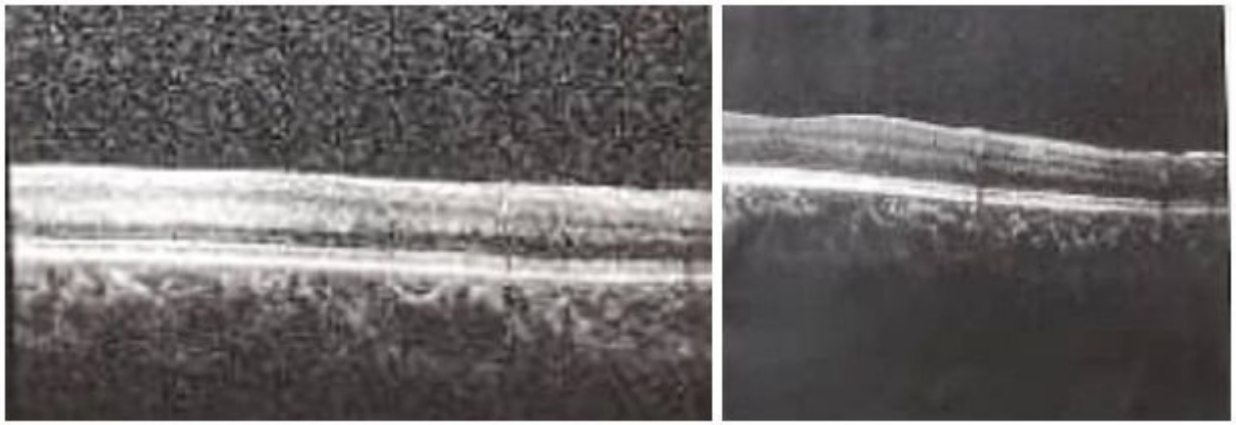

Figure 1

Optical Coherence Tomography (OCT) revealed a peripheral retinal edema and increased thickness of the retinal nerve fiber layer.

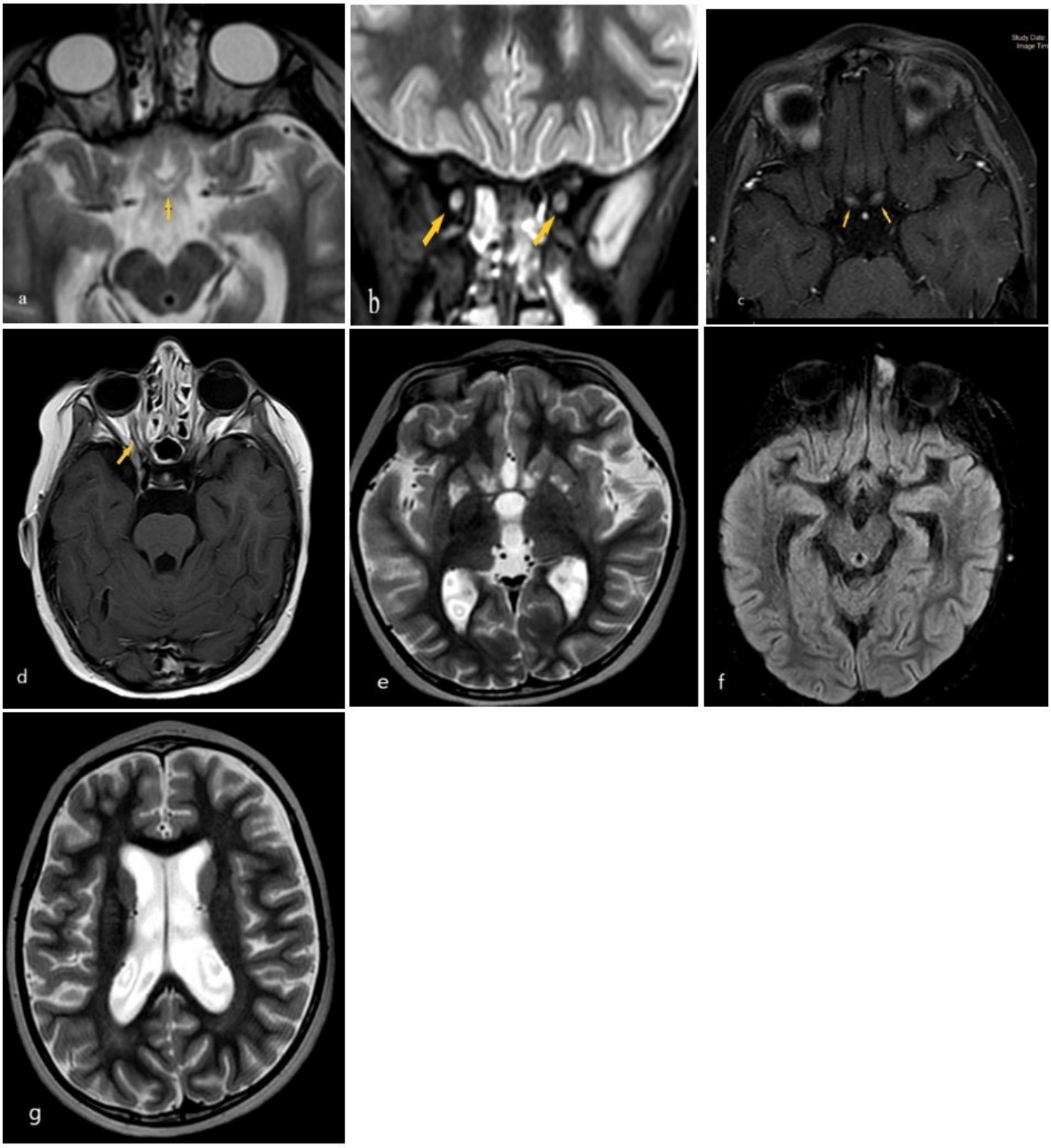

Figure 2

Brain and orbital MRI sequences of the first disease episode show abnormal signal intensity and enhancement of anterior optic pathways (yellow arrows in a to d), basal ganglia and periaqueductal involvement and mild general cerebral atrophy. (a) Abnormal signal intensity of optic chiasma on axial T2-W image, (b) Coronal STIR sequence is showing abnormal signal of bilateral intraorbital optic nerves, (c) Axial post contrast orbital T1-W +fat sat sequence is showing enhancement of bilateral intracranial

optic nerves, (d) Axial non-fat sat post contrast T1-W sequence shows enhancement of bilateral intra orbital optic nerves (yellow thin arrow), (e) Symmetric abnormal signal foci of basal ganglia on axial T2-W sequence, (f) Periaqueductal hypersignal intensity on axial FLAIR sequence and (g) Mild to moderate global cerebral atrophy on axial T2-W image associated with minimal hyperintensity in periventricular white matter

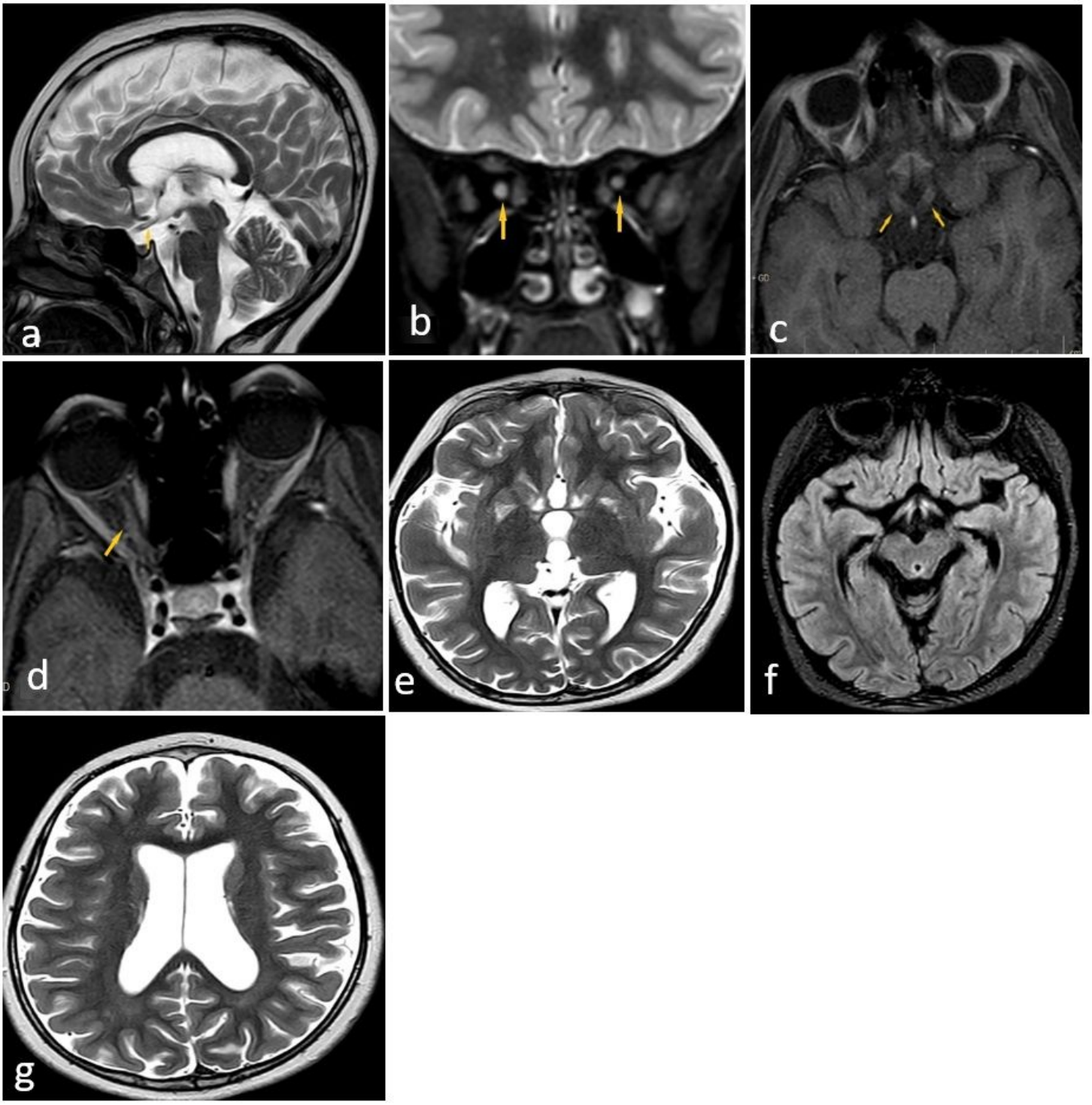

Figure 3

Brain and orbital MRI sequences of the second disease episode show the same changes of the first episode but the optic enhancement is milder than first episode (compare 1-b and 2-b). Abnormal signal intensity and enhancement of anterior optic pathways (yellow arrows in a to d), basal ganglia and periaqueductal involvement and general cerebral atrophy are still present. (a) Brain sagittal T2-W, (b) Orbital STIR, (c) and (d) Axial orbital and brain T1-W/fat sat with contrast administration, respectively. (e) and (g) Axial T2-W and (f) Axial FLAIR sequences shows progression in cerebral atrophy, basal ganglia signal changes and unchanged PAG involvement

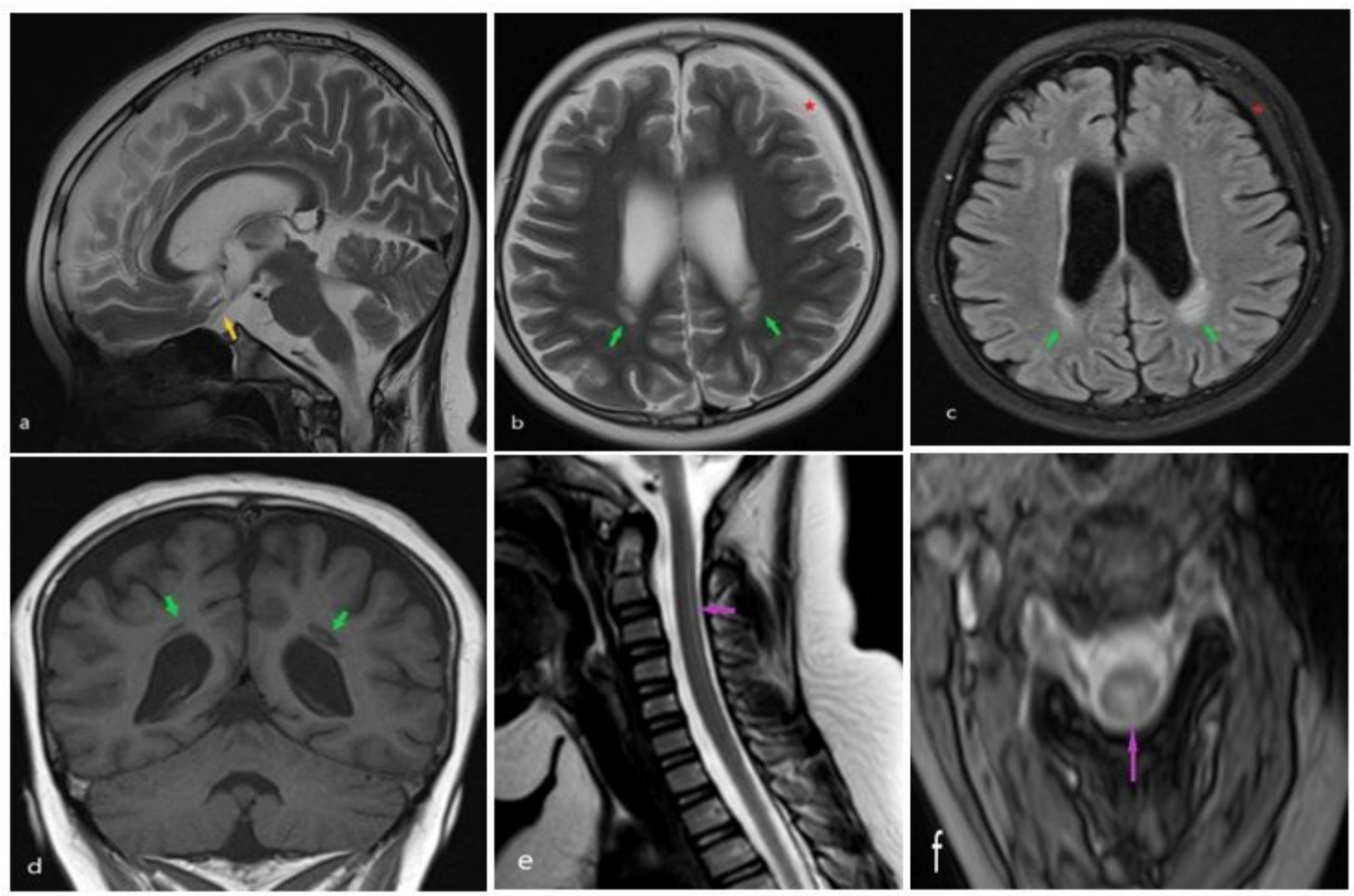

Figure 4

The brain MRI sequences at the time of third disease episode including sagittal and axial T2-W sequences, FLAIR (c) and coronal T1-W sequences (d) show additional optic nerve atrophy (yellow arrow in a) and increased periventricular white matter abnormal signal intensity (green arrows in b to d images) as well as thin chronic subdural hematoma (red stars in b and c) in left frontal extra-axial space compared to previous MRIs. Spinal MRI including sagittal and axial T2-w sequences (e and f) revealed long segment cervical cord involvement as hypersignal intensity mostly affecting its posterior aspect extending to upper thoracic cord (pink arrows).

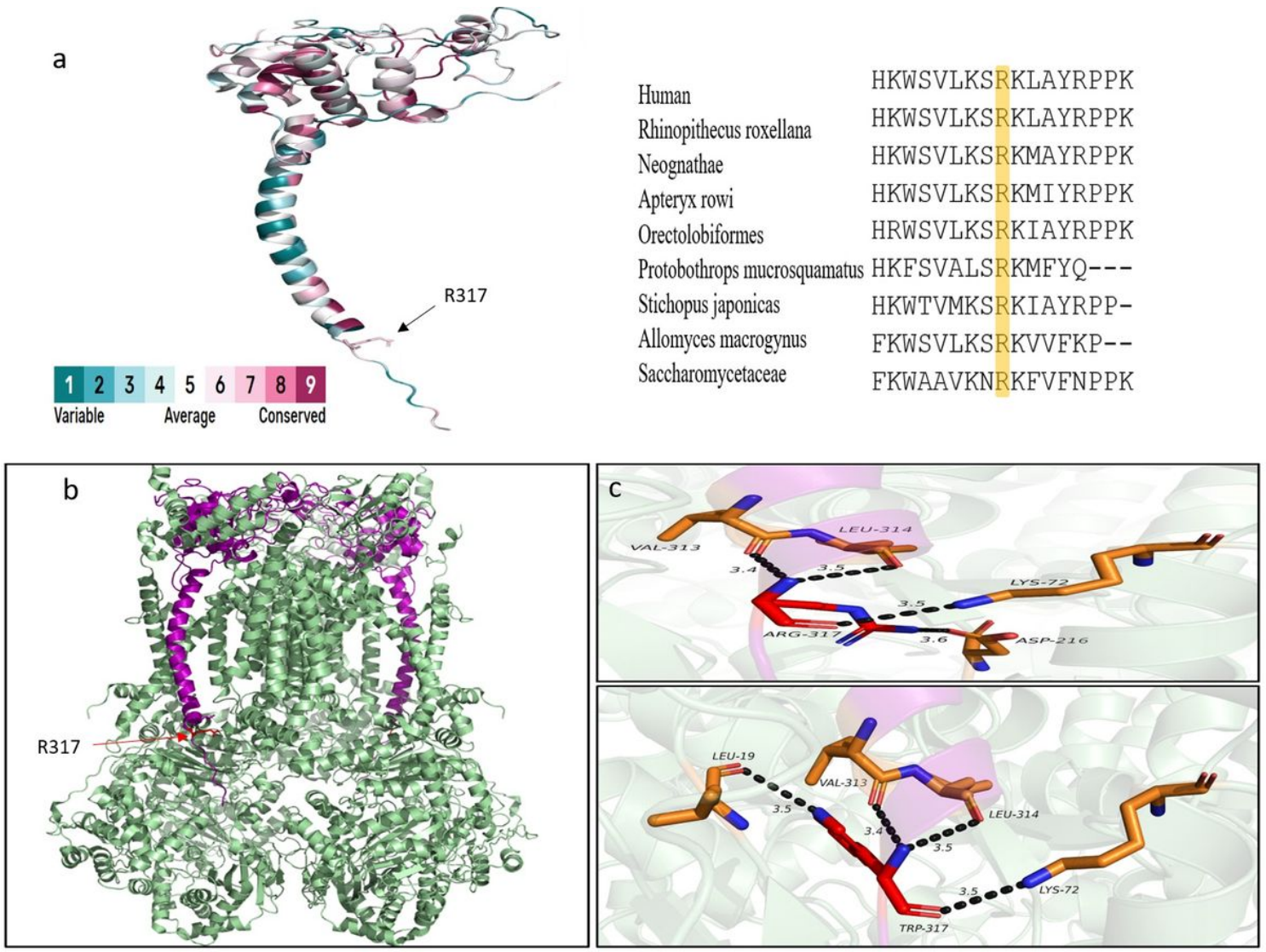

Figure 5

Conservation, Crystal structure of cytochrome c1 and polar contacts of native and mutated residue. (a) Left: Crystal structure of cyt c1 utilized for color-based demonstration of conservation (provided by Consurf). Right: UCSC database used to show the conservation status of a specific region including the variant site (highlighted in yellow). (b) The homodimer representation of cytochrome c1 (purple) within the complex III (green). (c) Protein modeling with pymol and effects of the identified variant on polar contacts with other atoms within the structure.